Structural Basis for Binding of Porphyrin to Human Telomeres[†,‡]

Gary N. Parkinson, Ragini Ghosh, and Stephen Neidle*

CRUK Biomolecular Structure Group, The School of Pharmacy, University of London, 29-39 Brunswick Square, London WC1N 1AX, United Kingdom

Received October 30, 2006; Revised Manuscript Received December 19, 2006

ABSTRACT: Maintenance of telomere integrity is a hallmark of human cancer, and the single-stranded 3′ ends of telomeric DNA are targets for small-molecule anticancer therapies. We report here the crystal structure of a bimolecular human telomeric quadruplex, of the sequence d(TAGGGTTAGGG), in a complex with the quadruplex-binding ligand 5,10,15,20-tetrakis(*N*-methyl-4-pyridyl)porphyrin (TMPyP4) to a resolution of 2.09 Å. The DNA quadruplex topology is parallel-stranded with external double-chain-reversal propeller loops, consistent with previous structural determinations. The porphyrin molecules bind by stacking onto the TTA nucleotides, either as part of the external loop structure or at the 5′ region of the stacked quadruplex. This involves stacked on hydrogen-bonded base pairs, formed from those nucleotides not involved in the formation of G-tetrads, and there are thus no direct ligand interactions with G-tetrads. This is in accord with the relative nonselectivity by TMPyP4 for quadruplex DNAs compared to duplex DNA. Porphyrin binding is achieved by remodeling of loops compared to the ligand-free structures. Implications for the design of quadruplex-binding ligands are discussed, together with a model for the formation of anaphase bridges, which are observed following cellular treatment with TMPyP4.

The 3′ ends of eukaryotic telomeric DNAs are single-stranded and comprise some 150−250 nucleotides of G-rich telomeric repeating DNA (*1*). The induction of the folding of these sequences into G-quadruplex structures by small-molecule ligands is being developed as an anticancer therapeutic strategy in humans (*2*, *3*). This is due to the ability of the resulting quadruplex−ligand complexes to inhibit telomerase, an enzyme central to cancer initiation and progression in almost all human cancers (*4*). G-Rich regions in promoter regions of a number of oncogenes have also been identified as being potentially capable of forming G-quadruplex structures (*5*−*7*), especially under the influence of appropriate ligands (*5*, *8*). These may then act as regulatory elements for gene expression. The porphyrin derivative TMPyP4[1] (Figure 1) has been extensively studied as a quadruplex-binding ligand since it induces telomerase inhibition upon binding to telomeric DNA quadruplexes (*9*−*11*). It also downregulates the expression of the oncogenes *c-myc* (*5*) and *k-ras* (*12*) on binding to the quadruplexes formed in their promoter sequences. The antitumor activity of TMPyP4 may be due to these effects (*8*). The stoichiometry and nature of the structure of porphyrin−quadruplex complexes have been controversial, and various models have been proposed, in large part on the basis of spectroscopic studies. These models involve TMPyP4 molecules in intercalative binding between adjacent G-tetrads (*13*, *14*), at a G-A interface (*15*), or stacked externally onto the end of a quadruplex (*13*, *16*). Of these, porphyrin intercalation between adjacent G-tetrads appears to be least favored on energetic grounds (*16*). Porphyrins have been shown to convert antiparallel quadruplex topologies into a parallel form (*17*). NMR solution studies of TMPyP4 complexed with a quadruplex formed from the *c-myc* promoter sequence (*18*, *19*) show a parallel-stranded topology for the DNA, with the TMPyP4 molecule situated at the end of the three-G-tetrad core of the quadruplex. TMPyP4, by contrast with other quadruplex-binding ligands such as telomestatin (*9*), does not have high selectivity for various quadruplex DNAs compared to duplex DNA (*20*, *21*).

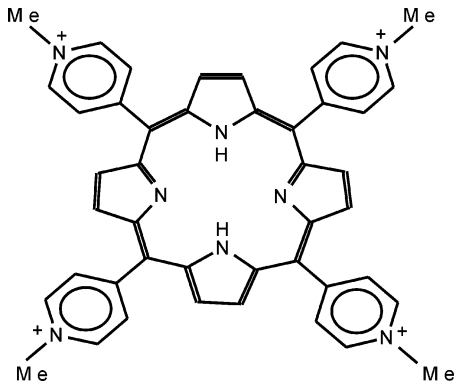

FIGURE 1: Structure of the TMPyP4 molecule.

The understanding of DNA G-quadruplex structure and topology is central to the design of ligands that can bind and stabilize them and thereby modulate particular cellular pathways and function. The structure and topology of quadruplexes based on repeats of the human telomeric sequence d(TTAGGG) have been studied by both X-ray (*22*) and NMR techniques (*23*−*26*). These data, together with

[†] This work was supported by Cancer Research UK (Programme Grant C129/A4489).

[‡] The atomic coordinates of d(TAGGGTTAGGG) complexed with TMPyP4 have been deposited in the Protein Data Bank as entry 2HRI.

* To whom correspondence should be addressed. Telephone: (44) 2077535969. Fax: (44)2077535970. E-mail: stephen.neidle@pharmacy.ac.uk.

[1] Abbreviation: TMPyP4, 5,10,15,20-tetrakis(*N*-methyl-4-pyridyl)-porphyrin.

10.1021/bi062244n CCC: $37.00
Published on Web 02/03/2007

information from biophysical studies (*27*, *28*), indicate that they can be conformationally heterogeneous in the presence of physiological levels of potassium ions. The structural studies have defined several different topologies. These range from all-parallel strands for bimolecular (two repeats) (*22*, *23*) and unimolecular, with four telomeric DNA repeats showing either all-parallel strands (*22*) or mixed parallel/antiparallel folding (*24*−*26*). These topologies also depend upon the number of repeats, the nature of the terminal nucleotides, and the chemical modification of the bases. The stability of the mixed folds appears to depend on the presence of additional base pairs arising from the presence of nontelomeric terminal residues (*25*, *26*). The apparently large number of native structures has hindered the determination and selection of optimal structural models for the design of ligands binding to human quadruplexes under physiologically relevant conditions. Thus, no crystal or detailed NMR structure of ligands bound to quadruplexes from human telomeric sequences has hitherto been reported. However, the cocrystal structure has been determined (*29*) for an acridine derivative bound within a diagonal T_4 loop of an antiparallel bimolecular quadruplex formed from the *Oxytricha nova* sequence d($G_4T_4G_4$). This has provided some structural data relevant to the design of relatively simple ligands, in demonstrating that the tricyclic acridine chromophore stacks directly onto the terminal G-tetrad of this quadruplex, and that the side chains are situated in the grooves.

We describe here the crystal structure of a complex of a bimolecular human telomeric G-quadruplex and the TMPyP4 molecule. The crystals have been grown in the presence of K^+ ions and reveal a parallel-stranded quadruplex with propeller loops that interact with two independent TMPyP4 molecules. This quadruplex topology is in accord with previous crystal structure and NMR determinations of bimolecular G-quadruplexes (*22*, *23*) containing the human telomeric repeat sequence d(TTAGGG). Loop residues from both strands interact by hydrogen bonding and base stacking to form a platform for ligand binding, resulting in the remodeling of both loop structures. The structure defines a novel binding mode for the porphyrin TMPyP4, since it is not directly in contact with the G-tetrads but stacked between base pairs that appear to be formed for ligand binding. This mode of interaction enables the TMPyP4 molecules to effectively stack between the bases without steric hindrance. This enables ligand−base $\pi-\pi$ interactions to be maximized, at an optimal separation of 3.4 Å, and electrostatic interactions to be optimized by interactions between the cationic substituent *N*-methylpyridinium groups and the phosphate ions.

MATERIALS AND METHODS

Crystallization. The DNA sequence d(TAGGGTTAGGG) was purchased from Eurogentec and used without further purification. The DNA samples were diluted into 2 mM stock solutions containing 20 mM potassium cacodylate buffer at pH 6.5 and 50 mM potassium chloride heated to 353 K for 10 min before being annealed overnight and cooled to room temperature. TMPyP4 was dissolved in 100% DMSO and diluted into water prior to use to give a 20 mM stock solution that was kept in the dark until it was used to avoid oxidation. It was mixed with the DNA at different molar ratios in the crystallization drops. Crystals were grown by vapor diffusion from hanging drops using molar mixing ratios of 1:1 to 5:1. The initial drop conditions included TMPyP4 together with 500 mM ammonium sulfate, 80 mM lithium sulfate, 80 mM sodium chloride, 80 mM potassium chloride, 20 mM potassium cacodylate, and 1 mM DNA, equilibrated against 1.4 M ammonium sulfate. Dark-brown crystals with dimensions of 0.3 mm × 0.2 mm × 0.2 mm grew within 1 week. Glycerol [25% (w/v) water] was required as a cryoprotectant to stabilize the crystals during freezing.

Table 1: X-ray Data Collection and Refinement Statistics

space group	$C222_1$
unit cell (Å)	$a = 37.29$, $b = 61.99$, $c = 61.40$
wavelength (Å)	1.5418
resolution range (Å)	28.35−2.09 (2.16−2.09)
total no. of reflections	22534
no. of unique reflections	4443
average redundancy[a]	5.07 (4.92)
completeness[a] (%)	99.9 (99.5)
mosaicity	1.03
R_{merge}[b]	0.043 (0.201)
reduced χ^2 [a]	0.98 (1.10)
output $\langle I/\sigma I\rangle$[a]	18.2 (6.5)
completeness for range (%)	99.82
no. of reflections	4239
R[c]	0.208
R_{free}	0.257
$\langle B\rangle$ (Å^2)	24.5
PDB entry	2HRI
content of asymmetric unit	22 nucleotides, 2.5 K^+ ions, 2 TMPyP4 ligands on 2-fold axes, 42 water molecules

[a] Highest-resolution shell in parentheses. [b] $R_{sym} = \sum_{hkl}|I(hkl) - \langle I(hkl)\rangle|/\sum I(hkl)$. [c] R-factor $= \sum_{hkl}||F_{obs}| - |F_{calc}||/\sum_{hkl}|F_{obs}|$. For the calculation of R_{free}, 5% of the test set amplitudes were employed, and these were not used in refinement.

Data Collection. Data were collected from flash-frozen crystals using an in-house RAXIS IV image-plate system and Osmic focusing mirrors. Data processing and reduction were carried out using DTREK (Rigaku). Table 1 summarizes the data collection and refinement statistics. The space group was determined to be $C222_1$ with cell dimensions consistent with two 11-mer strands per asymmetric unit.

Structure Solution and Refinement. The structure was determined by molecular replacement using PHASER (*30*) from the CCP4 package (*31*). Several parallel-stranded G-quadruplex models were used as potential search models. The molecular replacement model with the clearest solution was derived from the NMR structure of PDB entry 2A5R [a parallel-stranded G-quadruplex containing the *c-myc* promoter sequence in a complex with TMPyP4 (*18*)], with the lateral loop and three residues at the 5′ end removed. The initial electron density maps [calculated with TURBO-FRODO (*32*)] from this top solution confirmed the correct positioning of the three guanine quartet tetrads. The model was then refined with REFMAC (*33*), retaining the TMPyP4 ligand. In the initial round of refinement cycles, apparent electron density was observed in the plane of the ligand as well as two layers above, each separated by 3.5 Å, together with density for three K^+ ions. However, it became clear that the ligand molecule was not bound as in the starting model, above the top 5′ guanine tetrad, and the electron density maps above the G-tetrad could be best fitted using residues T12 and A13 from the 5′ end of the sequence of the B chain and residue A2 from the A chain, forming a base triad. Subsequent maps revealed two distinct binding

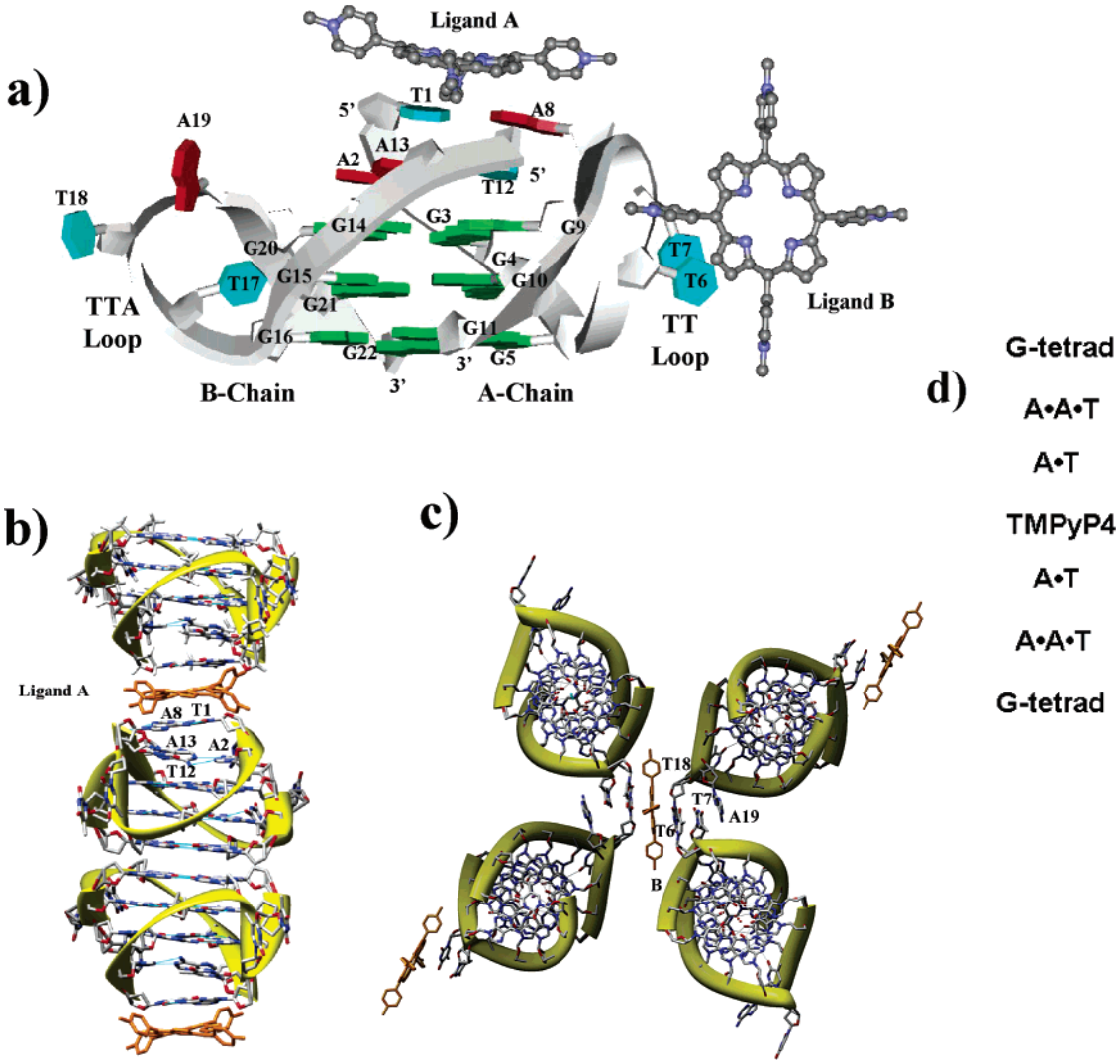

FIGURE 2: (a) Schematic view of the bimolecular quadruplex−TMPyP4 structure, showing the folding topology, the numbering of nucleotides, the extended TTA loop geometry, and the two TMPyP4 molecules bound per asymmetric unit. Guanine bases are colored green, adenines red, and thymines cyan. (b) View of a column of three consecutive quadruplexes as found in the crystal structure. Crystallographic 2-fold axes are midway between each quadruplex and are oriented toward the reader. (c) View of four symmetry-related quadruplex molecules in the crystal structure that generate the external loop-bound porphyrin binding pocket, viewed down the quadruplex columns. A crystallographic 2-fold axis is positioned at the center of this view, running through the loop-stacked TMPyP4 molecule shown at the center (yellow ball-and-stick representation). (d) Schematic of the stacking between adjacent quadruplexes, showing the base pairs, triplets, and G-tetrads on either side of the TMPyP4 molecule.

sites for the TMPyP4 molecule on crystallographic 2-fold axes, one centrally located between successive stacks of quadruplexes, sandwiched between two T·A base pairs, and the second stacked at right angles onto a T·T base pair, formed from the two external TTA loops.

RESULTS

Overall Features of the Structure. Two strands of the human telomeric repeat d(TAGGGTAGGG) associate together in the crystal structure to form an asymmetric parallel-stranded bimolecular quadruplex containing three planar stacked G-tetrads (Figure 2a), together with bound TMPyP4 ligand molecules (see below). Omit electron density maps (Figure 3c) show that both TMPyP4 molecules in the asymmetric unit are well-ordered. The parallel topology of the quadruplex is the same as that in the native human telomeric bimolecular and unimolecular structures previously determined crystallographically (*22*). Three monovalent K^+ cations are located between the tetrad planes in an antiprismatic bipyramidal arrangement, each coordinating to the O6 guanine substituent atoms in the central channel (Figure 3d), with the same geometry as in the native structure (*22*). The rmsd values between the structure presented here and these two structures, for the core guanine residues, are 1.21 and 1.67 Å, respectively. The connecting TTA nucleotides form a trinucleotide TTA and a dinucleotide TT external propeller loop, which connect the parallel G-rich strands together. These two loops are thus not equivalent, although both are also involved in stacking interactions with the ligands and, through crystal packing interactions, with each other.

Ligand Binding Geometry. The crystal structure consists of infinite stacks of TMPyP4−quadruplex complexes, with a 2-fold axis at each end of an individual quadruplex (Figure 2b). This results in each individual quadruplex being in an asymmetric environment such that (i) at one end it forms a quadruplex dimer by being stacked onto the quadruplex related by a crystallographic 2-fold symmetry element such that their two terminal G-quartets are 3.4 Å apart and have

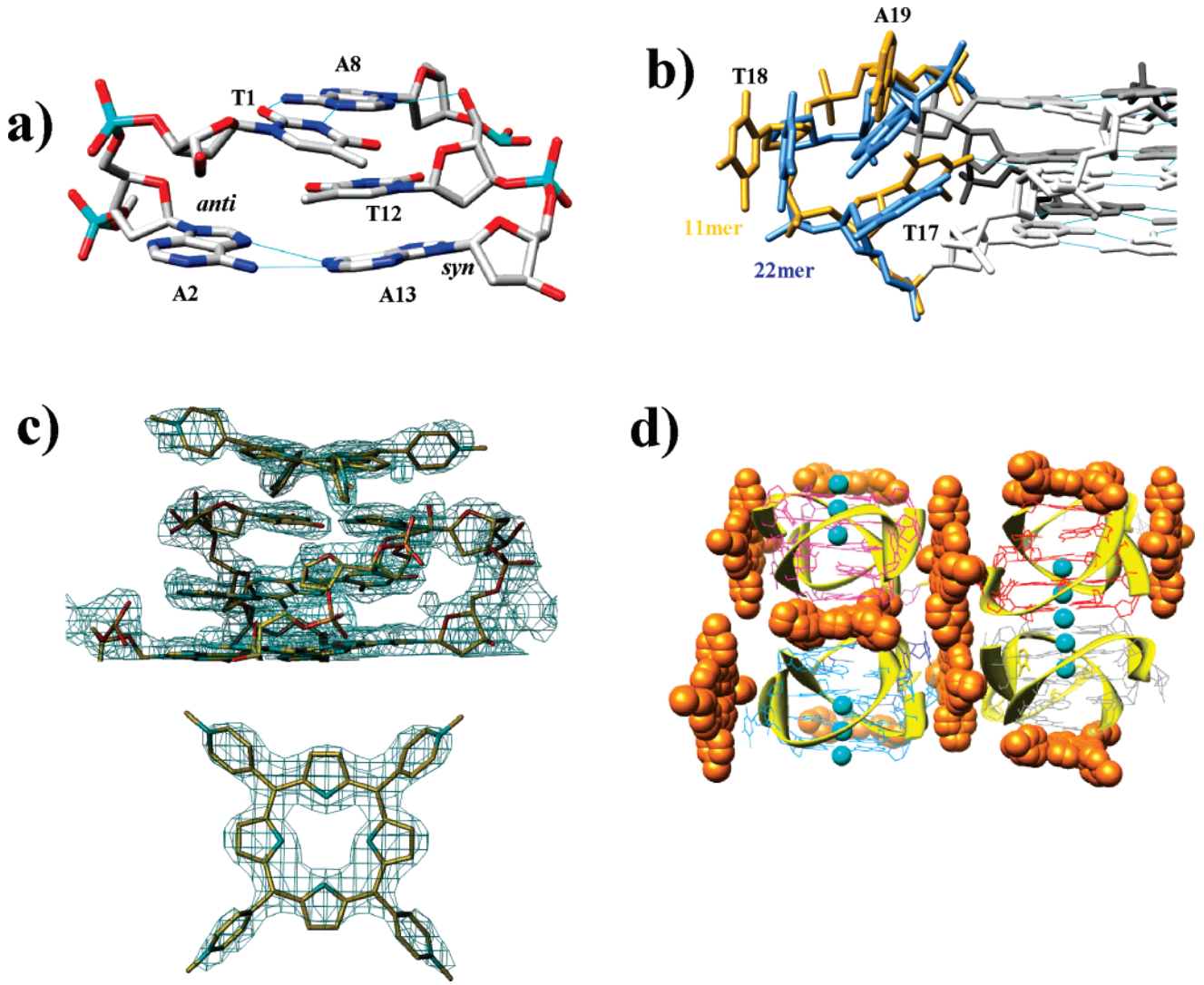

FIGURE 3: (a) View of the arrangement of the T1·A8 base pair stabilized below by the A2·A13·T12 triad that are stacked above the terminal G-tetrad in the structure. (b) Superposition of a TTA loop (blue) from the crystal structure of the native 22-mer (*22*) with the TTA loop (yellow) in the structure presented here. (c) A $2F_o - F_c$ electron density map (top) showing the TMPyP4 molecule stacked on top of the T·A base pair, drawn at a 1.2σ contour level with TURBO (*32*) and an omit map (bottom) showing electron density for the externally bound TMPyP4 molecule, drawn at a 2.2σ contour level. (d) View of the crystal structure along columns of the quadruplex−TMPyP4 complex, showing the porphyrin molecules in space-filling mode (colored orange), the quadruplex backbone (colored yellow), and the potassium ions (colored cyan).

a K^+ ion between them (coordinated to O6 guanine atoms from each quadruplex) and (ii) at the other end there is a TMPyP4 molecule (A), positioned on the adjacent 2-fold axis, sandwiched between the quadruplex and the next symmetry-related one.

The second TMPyP4 molecule (B) is perpendicular to the quadruplex stacks and interacts with the TTA loops in the crystal (Figure 2c). It also sits on a crystallographic 2-fold axis, which is perpendicular to the porphyrin plane, passing through the center of the TMPyP4 molecule. The interquadruplex-stacked TMPyP4 molecule has a nonplanar ruffled porphyrin core, whereas the core of the external loop-associated TMPyP4 molecule is planar. Both TMPyP4 molecules have their *N*-methyl-4-pyridyl groups oriented almost perpendicular to the mean porphyrin plane.

Unexpectedly, we find that TMPyP4 molecule A is not stacked either between or on any G-tetrads. Instead, it is stacked on a reverse Watson−Crick A·T base pair formed by the 5′ end T1 pairing with A8 from the same strand of the quadruplex. Hydrogen bond distances are as follows: 3.1 Å for the O2 T1···N6 A8 bond and 2.8 Å for the N3 T1···N1 A8 bond. This base pair is in turn situated above a loosely associated A2·T12·A13 base stepped-triad platform (Figure 3a) that arises from both strands. A 2-fold symmetry axis, through the porphyrin plane, results in a second A·T base pair on the other side of the porphyrin (Figure 2b) so that the TMPyP4 molecule is sandwiched between the two A·T pairs.

A8 is derived from one of the two extrahelical TTA loops, and its participation on this A·T base pair effectively reduces this loop to a TT dinucleotide one. The triad (Figure 3a) is formed from the 5′ end T12 and A13 of strand 2, together with A2 from strand 1, such that the two adenines form a buckled A·A base pair, involving the Hoogsteen face of A2 (in an anti conformation) and the Watson−Crick face of A13 (in a syn conformation). Hydrogen bond distances are as follows: 3.0 Å for the N6 A2···N1 A13 bond and 3.1 Å for the N7 A2···N6 A13 bond. T12, which is stepped up from the A·A plane and does not hydrogen bond to it, is also in a syn conformation. This positions its C5 methyl group to

be in the hydrophobic proximity of the C8 hydrogen atom of A2. T12 has A8 directly stacked above it. Both it and the A·A pair of the triad are also directly stacked on the other side onto the terminal G-tetrad (G3·G9·G14·G20) of the quadruplex so that the order of stacked planar groups is as shown in Figure 2d.

The two propeller loops protrude out from the stacked part of the structure. The TT loop has its two thymine nucleotides, T6 and T7, stacked one on another, and TMPyP4 molecule B is positioned in the space between the stacked quadruplexes in the crystal lattice such that one side of the porphyrin is stacked onto T6 (Figure 2c). This base forms a T·T base pair with the symmetry-related T18 from the other TTA loop so that this thymine also stacks on the porphyrin surface. Hydrogen bond distances are as follows: 2.8 Å for the O2 T6···N3 T18 bond and 3.0 Å for the N3 T6···N2 T18 bond. T7 from the TT loop is intercalated between T6 and A19. The other side of the flat porphyrin surface has a symmetry-related T·T pair stacked on it as a consequence of the 2-fold axis through the TMPyP4 (B) molecule so that all four of its pyrrole rings are sandwiched between the two T·T base pairs. One of the porphyrin *N*-methylpyridyl groups packs closely into the quadruplex backbone, close to the deoxyribose ring of G9.

Loop Structure. In all DNA quadruplex structures formed from the human telomeric repeat d(TTAGGG) that have been reported to date (*22*−*25*), the TTA trinucleotides form the connecting bridges between the guanine tracts which are involved in G-tetrad formation. The present quadruplex structure is formed from two strands, each containing two sets of three guanine repeats separated by only one full TTA repeat. This arrangement results in one connecting TTA loop per strand, and thus two loops per quadruplex. Here the two loops connecting the stacked tetrads together are dissimilar, unlike the previously determined crystal structures (*22*) for the human telomeric repeats. The TTA loop of the B chain has a structure similar to that of the previously determined propeller loop for the human telomeric sequence, both extending outward from the central guanine quartet. An additional hydrogen bonding contact (2.8 Å) is formed here, between O4 of T17 and N2 of G15, with the O4 replacing a potential water coordination site and stabilizing the propeller loop structure. This is a result of nucleotide T17 being turned inward toward the groove of the quadruplex. T18 extends the farthest out and is oriented parallel to A19, in accord with the previously observed loop structure (*22*). A comparison of the TTA propeller loop structures for strand 2 and the propeller loops of the previous crystal structures is shown in Figure 3b, highlighting the similarity of the folded loops. The two structures have been aligned using the central G-tetrads as a reference. The alignment of the backbone remains largely unchanged with the phosphate groups at 3′ and 5′ ends overlapping, highlighting the similarity of the quadruplex structures. Several small but significant modifications to base geometry can be seen in the loop region. The largest shift occurs to T17 which is no longer stacked but turned inward toward the quadruplex groove, while T18 and A19 are rotated to accommodate the intercalation of T6 from strand 1. T18 is pushed farther out with only a small rotation of A19. In contrast, the A chain TT loop has a compressed propeller loop topology, as A8 is stacked along the axis of the quadruplex, between T12, located at the 5′ end of the quadruplex while T6 and T7 project outward away from the grooves. Although the two loop structures are very different, the overall topology of the quadruplex is retained, with overlapping of the phosphates at the 3′ and 5′ ends.

Hydration Structure. Within the grooves of DNA crystal structures, ordered hydration structures are usually observed. In both this TMPyP4 complex and the native (*22*) crystal structures with all-parallel stranded G-quadruplexes, where all guanosine nucleosides have the same anti glycosidic torsion angle, four equivalent external grooves are generated that are lined by N2 amino and N3 atoms of the guanine bases. These form the floor of the grooves to define a scaffold for hydration. The majority of the guanines have their N2 and N3 atoms coordinated to solvent atoms, as they do in the native human telomeric quadruplex crystal structures (*22*). Those water molecules coordinating to N2 are close to the G-tetrad planes, while waters coordinating to N3 lie either above or below these planes. Additional points of contact come from the sugar O4′ atoms on the groove walls, which expand the scope of the hydration networks and can be involved in forming a bridge from them to the N3 atoms in the grooves. The networks are further extended through phosphate backbone contacts, although water molecules between adjacent phosphates were not observed. The points of hydration also define potential sites for hydrogen bonding and stabilization, as observed in the case of the O4 substituent of T17 displacing a water molecule and hydrogen bonding to the N2 atom of G15, and also stabilizing T17 in the groove (Figure 3b).

DISCUSSION

The G-rich single-stranded overhang of telomeric DNAs, being unconstrained by the stereochemical requirements of the double helix, can readily fold into G-quadruplex DNA structures, subject only to competition with the single-stranded binding protein hPOT1 and telomerase (*34*). It has been shown that small molecules can effectively compete with hPOT1 and thus can stabilize quadruplex−ligand complexes at the 3′ telomeric end (*35*). In principle, such complexes can involve either unimolecular (from folding of the one strand) or bimolecular quadruplexes from two telomeres associating together. The crystal structure presented here shows how one such ligand, the porphyrin molecule TMPyP4, can bind to such a bimolecular human telomeric quadruplex; this ligand has been reported to have a preference for stabilizing bimolecular rather than unimolecular quadruplexes (*9*). Previous studies on TMPyP4 telomeric quadruplex complexes have been interpreted as suggesting a binding mode in which a ligand molecule stacks directly onto the G-tetrad core. This is not observed here. Instead, two rather different binding modes are seen in this ligand−quadruplex complex, with both bound ligand molecules contacting only bases from the TTA loops, albeit in very different ways. One TMPyP4 molecule is stacked onto a A·T base pair that is formed from the 5′ end thymine, and from an adenine derived from conformational reorganization of one of the TTA loops, so that it becomes a TT propeller loop. There are no direct ligand contacts with any G-tetrads (and no TMPyP4 intercalation between adjacent G-tetrads, as suggested by some previous models). This is a consequence of the need to avoid any steric hindrance that arises from the *N*-methylpyridyl

groups of TMPyP4, which are oriented out of the porphryin plane. The width across a G-tetrad at its narrowest point is ca. 11 Å, whereas the planar porphyrin core of the TMPyP4 molecule is only ca. 10 Å so that steric clashes between G-tetrad edges and the *N*-methylpyridyl groups would occur if the TMPyP4 molecule were to be stacked 3.4 Å above a G-tetrad.

The second TMPyP4 molecule is stacked externally onto thymine bases at the edges of both the TTA and TT loops. The environment of the crystal structure provides intermolecular contacts between quadruplexes (Figure 3d), to form, for example, the T·T base pairs, enhancing the stabilization of these externally bound ligand molecules. However, some association with the loops could be expected even in free solution, in accord with recent observations suggestive of a porphyrin external binding mode (*41*). Loop interactions have not been considered up till now in the design of quadruplex-binding ligands; these features in our structure suggest that their exploitation may provide a route to enhanced selectivity.

The two earlier crystallographic studies on binding of TMPyP4 to duplex DNA have found limited stacking and pseudo-intercalative modes of binding, demonstrating the ability of the porphyrin core to be in effective $\pi-\pi$ contact with base pairs. In one structure, a copper-containing TMPyP4 ligand has been shown to intercalate into a stacked B-DNA duplex, displacing a cytosine (*36*). In the second structure (*37*), a buckled nickel−porphyrin molecule stacks onto a base pair at the end of the DNA duplex and also groove binds to a symmetry-related DNA molecule. Both independent TMPyP4 molecules in this crystal structure demonstrate analogous $\pi-\pi$ stacking onto base pairs.

The NMR structure (*18*) of a parallel-stranded G-quadruplex from the *c-myc* promoter sequence complexed with TMPyP4 provides some analogies to the present structure, although the ligand has been modeled in the *c-myc* complex to be stacked on the external face of the terminal G-tetrad. However, steric hindrance is evident as the position of the porphyrin ring is 4.2 Å above the G-tetrad plane, which is considerably greater than the normal 3.4 Å $\pi-\pi$ stacking distance. We conclude that the steric restraints inherent in the TMPyP4 molecule can accommodate effective stacking with base pairs, but not with the more stringent requirements imposed by a G-tetrad. A number of porphyrin and TMPyP4 derivatives have been examined for quadruplex affinity and telomerase inhibition (*20*, *21*, *38*−*42*). Quantitative duplex affinity data are available only for some of these compounds and with some quadruplex sequences (see, for example, refs *20* and *21*); there is a clear trend of comparable quadruplex and duplex binding for most porphyrins. This is consistent with the structural data presented here, that porphyrins bind to the base pairs rather than the G-tetrad moieties within quadruplexes, consistent with the observations in solution of a lack of specificity with respect to duplex DNA.

We have previously suggested (*43*) that the difference in total surface area between G-tetrads in quadruplex and base pairs in duplex DNA is one factor that can be exploited for the design of quadruplex-selective ligands. The structure presented here indicates that the TMPyP4 molecule is unable to do this and thus may not be an optimal platform for future ligand design. More complex quadruplex-binding molecules such as the selenosapphyrin derivative (*40*), an expanded porphyrin, or neomycin-capped molecules (*44*) do show enhanced quadruplex selectivity, which may well be a consequence of their substantial nonplanar structures being able to interact with the structurally more complex loop regions rather than having selectivity through $\pi-\pi$ stacking.

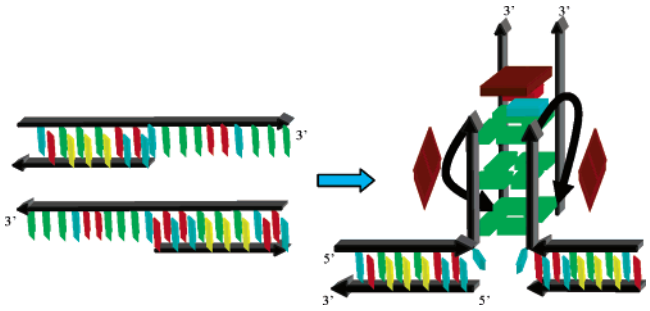

FIGURE 4: Schematic representation of a possible model for the formation of anaphase bridges, via quadruplex structures joining two separate 3′ single-stranded telomeric DNA chromosomal ends, and stabilized by TMPyP4 (shown as rectangles).

The structure presented here shows that the stable parallel quadruplex topology, seen in the native crystal structures (*22*), is preserved on ligand binding. However, the requirements imposed by a particular ligand (here, TMPyP4) have forced a major change in one loop, from a trinucleotide TTA loop to a dinucleotide TT one, which ensures that an adenine becomes available on top of the G-tetrad face. In general, shorter loops may enhance the stability of the parallel topology (*45*−*47*) since they are too short to form effective diagonal or lateral loops. Thus, the core quadruplex motif clearly provides a stable scaffold, but it is the loops that have the flexibility and diversity of interaction surfaces to bind to the porphyrin. Whether the topology of the native human telomeric sequence is in an all-parallel (*22*, *23*) or a mixed parallel/antiparallel arrangement (*25*−*27*) may be less relevant than a loop topology that can be flexible enough to provide a more complex and flexible interface for the binding of large molecules such as TMPyP4. Thus, other large ligands with distinct structures (*40*, *44*) may well induce different loop arrangements. The remodeling of the propeller loops under the influence of TMPyP4 demonstrates the flexibility available to the TTA nucleotides even when they are anchored at the 3′ and 5′ ends. These nucleotides utilize hydrogen bonding, base stacking, and intercalation to form the interaction surfaces needed for binding the TMPyP4 molecule. We cannot totally discount a possible role played by the close packing environment in the remodeling of these loops since this crystal structure also shows how individual quadruplex DNA molecules can associate tightly together in the presence of particular ligands, as shown in Figure 3d. However, the steric constraints imposed by the TMPyP4 molecule itself within an individual quadruplex are likely to dominate.

The known tendency of TMPyP4 to stabilize bimolecular rather than unimolecular quadruplexes may be relevant to its ability both to inhibit telomerase and to induce the formation of anaphase bridges at the ends of telomeres (*9*). The crystal structure presented here also provides the basis for a model for bridge formation and TMPyP4 stabilization, in which two separate chromosomes are linked with the formation and stabilization of a strand from each single-stranded overhang to form a parallel bimolecular quadruplex that is held together by porphyrin binding (Figure 4).

REFERENCES

1. McEachern, M. J., Krauskopf, A., and Blackburn, E. H. (2000) Telomeres and their control, *Annu. Rev. Genet. 34*, 331−358.
2. Neidle, S., and Parkinson, G. N. (2002) Telomere maintenance as a target for anticancer drug discovery, *Nat. Rev. Drug Discovery 1*, 383−393.
3. Kelland, L. R. (2005) Overcoming the immortality of tumour cells by telomere and telomerase based cancer therapeutics: Current status and future prospects, *Eur. J. Cancer 41*, 971−979.
4. Shay, J. W. and Wright, W. E. (2006) Telomerase therapeutics for cancer: Challenges and new directions, *Nat. Rev. Drug Discovery 5*, 577−584.
5. Siddiqui-Jain, A., Grand, C. L., Bearss, D. J., and Hurley, L. H. (2002) Direct evidence for a G-quadruplex in a promoter region and its targeting with a small molecule to repress c-*MYC* transcription, *Proc. Natl. Acad. Sci. U.S.A. 99*, 11593−11598.
6. Rankin, S., Reszka, A. P., Huppert, J., Zloh, M., Parkinson, G. N., Todd, A. K., Ladame, S., Balasubramanian, S., and Neidle, S. (2005) Putative DNA quadruplex formation within the human c-kit oncogene, *J. Am. Chem. Soc. 127*, 10584−10589.
7. Dexheimer, T. S., Sun, D., and Hurley, L. H. (2006) Deconvoluting the structural and drug-recognition complexity of the G-quadruplex-forming region upstream of the bcl-2 P1 promoter, *J. Am. Chem. Soc. 128*, 5404−5415.
8. Lemarteleur, T., Gomez, D., Paterski, R., Mandine, E., Mailliet, P., and Riou, J. F. (2004) Stabilization of the c-myc gene promoter quadruplex by specific ligands' inhibitors of telomerase, *Biochem. Biophys. Res. Commun. 323*, 802−808.
9. Kim, M. Y., Gleason-Guzman, M., Izbicka, E., Nishioka, D., and Hurley, L. H. (2003) The different biological effects of telomestatin and TMPyP4 can be attributed to their selectivity for interaction with intramolecular or intermolecular G-quadruplex structures, *Cancer Res. 63*, 3247−3256.
10. Izbicka, E., Wheelhouse, R. T., Raymond, E., Davidson, K. K., Lawrence, R. A., Sun, D., Windle, B. E., Hurley, L. H., and Von Hoff, D. D. (1999) Effects of cationic porphyrins as G-quadruplex interactive agents in human tumor cells, *Cancer Res. 59*, 639−644.
11. Grand, L. C., Han, H., Munoz, R. M., Weitman, S., Von Hoff, D. D., Hurley, L. H., and Bearss, D. J. (2002) The cationic porphyrin TMPyP4 down-regulates *c-myc* and human telomerase reverse transcriptase expression and inhibits tumor growth *in vivo*, *Mol. Cancer Ther. 1*, 566−573.
12. Cogoi, S., and Xodo, L. E. (2006) G-quadruplex formation within the promoter of the KRAS proto-oncogene and its effect on transcription, *Nucleic Acids Res. 34*, 2536−2549.
13. Wei, C., Jia, G., Yuan, J., Feng, Z., and Li, C. (2006) A spectroscopic study on the interactions of porphyrin with G-quadruplex DNAs, *Biochemistry 45*, 6681−6691.
14. Keating, L. R., and Szalai, V. A. (2004) Parallel-stranded guanine quadruplex interactions with a copper cationic porphyrin, *Biochemistry 43*, 15891−15900.
15. Mita, H., Ohyama, T., Tanaka, Y., and Yamamoto, Y. (2006) Formation of a complex of 5,10,15,20-tetrakis(N-methylpyridinium-4-yl)-21H,23H-porphyrin with G-quadruplex DNA, *Biochemistry 45*, 6765−6772.
16. Han, H., Langley, D. R., Rangan, A., and Hurley, L. H. (2001) Selective interactions of cationic porphyrins with G-quadruplex structures, *J. Am. Chem. Soc. 123*, 8902−8913.
17. Arthanari, H., and Bolton, P. H. (1999) Porphyrins can catalyze the interconversion of DNA quadruplex structural types, *Anticancer Drug Des. 14*, 317−326.
18. Phan, A. T., Kuryavyi, V., Gaw, H. Y., and Patel, D. J. (2005) Small-molecule interaction with a five-guanine-tract G-quadruplex structure from the human MYC promoter, *Nat. Chem. Biol. 1*, 167−173.
19. Hurley, L. H., Von Hoff, D. D., Siddiqui-Jain, A., and Yang, D. (2006) Drug targeting of the c-MYC promoter to repress gene expression via a G-quadruplex silencer element, *Semin. Oncol. 33*, 498−512.
20. Ren, J., and Chaires, J. B. (1999) Sequence and structural selectivity of nucleic acid binding ligands, *Biochemistry 38*, 16067−16075.
21. Wang, P., Ren, L., He, H., Liang, F., Zhou, X., and Tan, Z. (2006) A phenol quaternary ammonium porphyrin as a potent telomerase inhibitor by selective interaction with quadruplex DNA, *ChemBioChem 7*, 1155−1159.
22. Parkinson, G. N., Lee, M. P. H., and Neidle, S. (2002) Crystal structure of parallel quadruplexes from human telomeric DNA, *Nature 417*, 876−880.
23. Phan, A. T., and Patel, D. J. (2003) Two-repeat human telomeric d(TAGGGTTAGGGT) sequence forms interconverting parallel and antiparallel G-quadruplexes in solution: Distinct topologies, thermodynamic properties, and folding/unfolding kinetics, *J. Am. Chem. Soc. 125*, 15021−15027.
24. Wang, Y., and Patel, D. J. (1993) Solution structure of the human telomeric repeat d[$AG_3(T_2AG_3)_3$] G-tetraplex, *Structure 1*, 263−282.
25. Ambrus, A., Chen, D., Dai, J., Bialis, T., Jones, R. A., and Yang, D. (2006) Human telomeric sequence forms a hybrid-type intramolecular G-quadruplex structure with mixed parallel/antiparallel strands in potassium solution, *Nucleic Acids Res. 34*, 2723−2735.
26. Luu, K. N., Phan, A. T., Kuryavyi, V., Lacroix, L., and Patel, D. J. (2006) Structure of the human telomere in K^+ solution: An intramolecular (3 + 1) G-quadruplex scaffold, *J. Am. Chem. Soc. 128*, 9963−9970.
27. Xu, Y., Noguchi, Y., and Sugiyama, H. (2006) The new models of the human telomere d[$AGGG(TTAGGG)_3$] in K^+ solution, *Bioorg. Med. Chem. 14*, 5584−5591.
28. Ying, L., Green, J. J., Li, H., Klenerman, D., and Balasubramanian, S. (2003) Studies on the structure and dynamics of the human telomeric G quadruplex by single-molecule fluorescence resonance energy transfer, *Proc. Natl. Acad. Sci. U.S.A. 100*, 14629−14634.
29. Haider, S. M., Parkinson, G. N., and Neidle, S. (2003) Structure of a G-quadruplex-ligand complex, *J. Mol. Biol. 326*, 117−125.
30. McCoy, A. J., Grosse-Kunstleve, R. W., Storoni, L. C., and Read, R. J. (2005) Likelihood-enhanced fast translation functions, *Acta Crystallogr. D61*, 458−464.
31. The CCP4 Suite: Programs for Protein Crystallography (1995) *Acta Crystallogr. D50*, 760−763.
32. Cambillau, C., and Horjales, E. (1987) TOM: A FRODO subpackage for protein-ligand fitting with interactive energy minimization, *J. Mol. Graphics 5*, 175−177.
33. Murshudov, G. N., Vagin, A. A., and Dodson, E. J. (1997) Refinement of macromolecular structures by the maximum-likelihood method, *Acta Crystallogr. D53*, 240−255.
34. Zaug, A. J., Podell, E. R., and Cech, T. R. (2005) Human POT1 disrupts telomeric G-quadruplexes allowing telomerase extension in vitro, *Proc. Natl. Acad. Sci. U.S.A. 102*, 10864−10869.
35. Gomez, D., O'Donohue, M.-F., Wenner, T., Douarre, C., Macadré, J., Koebel, P., Giraud-Panis, M.-J., Kaplan, H., Kolkes, A., Shinya, K., and Riou, J.-F. (2006) The G-quadruplex ligand telomestatin inhibits POT1 binding to telomeric sequences in vitro and induces GFP-POT1 dissociation from telomeres in human cells, *Cancer Res. 66*, 6908−6912.
36. Lipscomb, L. A., Zhou, F. X., Presnell, S. R., Woo, R. J., Peek, M. E., Plaskon, R. R., and Williams, L. D. (1996) Structure of DNA-porphyrin complex, *Biochemistry 35*, 2818−2823.
37. Bennett, M., Krah, A., Wien, F., Garman, E., McKenna, R., Sanderson, M., and Neidle, S. (2000) A DNA-porphyrin minor-groove complex at atomic resolution: The structural consequences of porphyrin ruffling, *Proc. Natl. Acad. Sci. U.S.A. 97*, 9476−9481.
38. Shi, D.-F., Wheelhouse, R. T., Sun, D., and Hurley, L. H. (2001) Quadruplex-interactive agents as telomerase inhibitors: Synthesis of porphyrins and structure-activity relationship for the inhibition of telomerase, *J. Med. Chem. 44*, 4509−4523.
39. Dixon, I. M., Lopez, F., Estève, J.-P., Tejera, A. M., Blasco, M. A., Pratviel, G., and Meunier, B. (2004) Porphyrin derivatives for telomere binding and telomerase inhibition, *ChemBioChem 6*, 123−132.
40. Seenisamy, J., Bashyam, S., Gokhale, V., Vankayalapati, H., Sun, D., Siddiqui-Jain, A., Streiner, N., Shin-ya, K., White, E., Wilson, W. D., and Hurley, L. H. (2005) Telomestatin and diseleno sapphyrin bind selectively to two different forms of the human telomeric G-quadruplex structure, *J. Am. Chem. Soc. 127*, 9439−9447.

41. Yamashita, T., Uno, T., and Ishikawa, Y. (2005) Stabilization of guanine quadruplex DNA by the binding of porphyrins with cationic side arms, *Bioorg. Med. Chem. 13*, 2423−2430.
42. Goncalves, D. P., Ladame, S., Balasubramanian, S., and Sanders, J. K. (2006) Synthesis and G-quadruplex binding studies of new 4-N-methylpyridinium porphyrins, *Org. Biomol. Chem. 4*, 3337−3342.
43. Read, M., Harrison, R. J., Romagnoli, B., Tanious, F. A., Gowan, S. H., Reszka, A. P., Wilson, W. D., Kelland, L. R., and Neidle, S. (2001) Structure-based design of selective and potent G quadruplex-mediated telomerase inhibitors, *Proc. Natl. Acad. Sci. U.S.A. 98*, 4844−4849.
44. Kaiser, M., De Cian, A., Sainlos, M., Renner, C., Mergny, J.-L., and Teulade-Fichou, M. P. (2006) Neomycin-capped aromatic platforms: Quadruplex DNA recognition and telomerase inhibition, *Org. Biomol. Chem. 4*, 1049−1057.
45. Hazel, P., Huppert, J., Balasubramanian, S., and Neidle, S. (2004) Loop-length-dependent folding of G-quadruplexes, *J. Am. Chem. Soc. 126*, 16405−16415.
46. Hazel, P., Parkinson, G. N., and Neidle, S. (2006) Predictive modeling of topology and loop variations in dimeric DNA quadruplex structures, *Nucleic Acids Res. 34*, 2117−2127.
47. Burge, S. E., Parkinson, G. N., Hazel, P., Todd, A. K., and Neidle, S. (2006) Quadruplex DNA: Sequence, topology and structure, *Nucleic Acids Res. 34*, 5402−5415.

BI062244N